DifuzCam: Replacing Camera Lens with a Mask and a Diffusion Model

Erez Yosef
Tel Aviv University, Israel
erez.yo@gmail.com

Raja Giryes
Tel Aviv University, Israel
raja@tauex.tau.ac.il

Abstract

The flat lensless camera design reduces the camera size and weight significantly. In this design, the camera lens is replaced by another optical element that interferes with the incoming light. The image is recovered from the raw sensor measurements using a reconstruction algorithm. Yet, the quality of the reconstructed images is not satisfactory. To mitigate this, we propose utilizing a pre-trained diffusion model with a control network and a learned separable transformation for reconstruction. This allows us to build a prototype flat camera with high-quality imaging, presenting state-of-the-art results in both terms of quality and perceptuality. We demonstrate its ability to leverage also textual descriptions of the captured scene to further enhance reconstruction. Our reconstruction method which leverages the strong capabilities of a pre-trained diffusion model can be used in other imaging systems for improved reconstruction results.

1. Introduction

Cameras have become very popular and common in recent years, especially in small handheld devices. Despite that, reducing the size of the camera remains a difficult problem since a camera requires lenses and optical elements to get a high-quality image. Flat cameras [43] is a computational photography method to reduce camera size by replacing the camera lens with a diffuser, namely, an amplitude mask placed very close to the sensor. Thus, the image on the sensor consists of multiplexed projections of the scene reflections on all the sensors area such that the captured image is not visually understandable. Using a computational algorithm, the scene image can be retrieved. Yet, while achieving massive camera size reduction, reconstructing high-quality images from flat camera measurements is an ill-posed task and hard to achieve.

Previous approaches tried to reconstruct the scene image using different techniques including direct optimiza-

(a) Prototype flat camera (b) Captured image
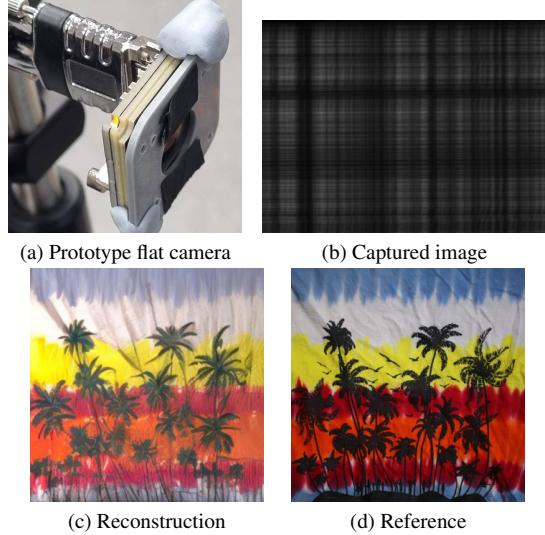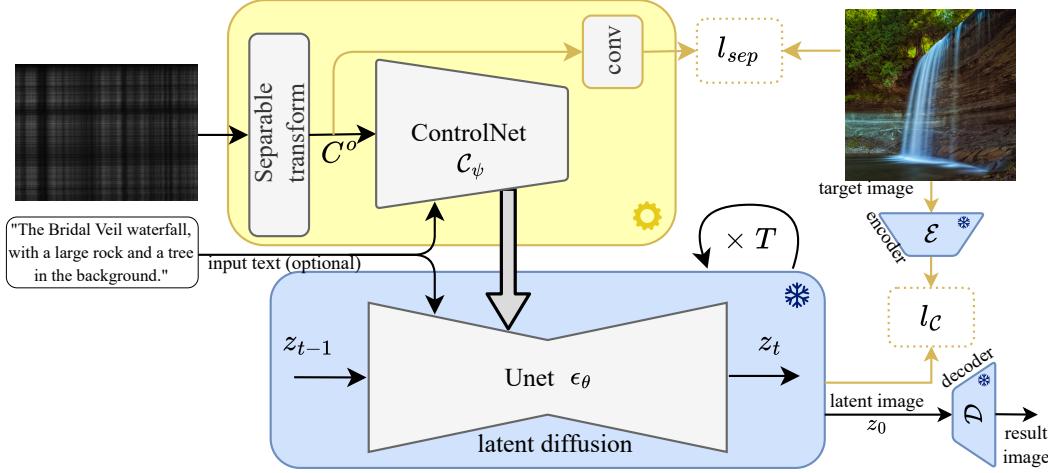
(c) Reconstruction (d) Reference

Figure 1. Using (a) our prototype flat camera, (b) a measurement image is captured that is not visually understandable. (c) An image is reconstructed from the measurements using our text-guided approach. Compare to (d) the reference image captured with a regular camera. (see Figure 7 for details).

tion [43] and deep learning [20]. Despite these attempts, the resulting images are not of sufficient quality. High-quality image reconstruction from flat camera measurements is still not solved and better algorithms are required to reproduce better images.

We propose *DifuzCam*, a novel strategy for flat camera image reconstruction using a strong image prior that relies on a pre-trained diffusion model [9, 38]. An overview diagram of DifuzCam is presented in Figure 2. Using a pre-trained image generation model, which is trained on a huge amount of images, we utilize a strong prior for natural images perceptually. This facilitates reconstructing state-of-the-art quality images from flat camera measurements (Figure 1b). Moreover, we leveraged the diffusion model text-guidance property for generation to improve even further image reconstruction through a description of the captured scene from the photographer.

Figure 2. **DifuzCam Proposed Method.** A flat lensless camera measurements are inputted to a separable linear transformation followed by a ControlNet adapter to control the image generation process by a pre-trained latent diffusion model (LDM). Using text guidance for the reconstruction process is optional in our method. On training, the **yellow** blocks weights are optimized, and **orange** paths are the training losses, while the **blue** blocks weights are pre-trained and fixed. The dataset for training and tests was captured using our prototype flat camera by projecting images onto a screen. We present an additional loss l_{sep} in addition to the diffusion training loss ($l_{\mathcal{C}}$) for better convergence. Reconstructed image is achieved by T iterative diffusion steps and decoding from latent space to pixel space.

We used stable diffusion [38] and trained a ControlNet [51] for our flat camera images captured by our flat camera prototype (Figure 1a). We present qualitative and quantitative evaluations of our proposed method using both our camera prototype and existing datasets from prior work to perform a comparison.

The method we present improves the reconstruction from flat camera measurements and thus, makes these cameras more practical. Additionally, our proposed approach can be modified for other imaging systems and setups. It leverages the diffusion model's strong prior and text guidance capability to improve the reconstructed image quality.

To conclude, our main contributions are: (i) A novel computational photography method based on a lensless flat camera and a reconstruction algorithm based on diffusion model image prior; (ii) State-of-the-art results for flat camera reconstruction quality in all evaluated metrics; (iii) A novel approach to using text guidance to improve imaging results of an optical system; and (iv) We present a deep control network with intermediate separable loss for improving convergence and results.

2. Related Work

Lensless imaging has garnered significant attention in recent years since it offers a more compact, light, and cost-effective imaging system. Different approaches to lensless camera design were proposed, such as static amplitude mask [43], modulation with LCD [18], Fresnel zone aperture (FZA) with SLM [11, 29, 45], phase mask [3, 6], programmable devices [17, 27, 53, 55], and more as described

in the following review [7].

In this paper, we rely on the FlatCam design [43]. It employs a static amplitude mask placed near the sensor. The mask pattern is designed in a separable manner such that the imaging linear model can be simplified to a separable operation:

$$Y = \Phi_l X \Phi_r, \qquad (1)$$

where Φ_L and Φ_R are the separable operations on the image's rows and columns, respectively. X is the scene intensity and Y is the sensor measurements.

In this case, the measurements of the camera consist of multiplexed projections of the scene reflectance such that reconstruction becomes an ill-posed problem. Prior methods for image reconstruction from flat camera measurements were designed as an optimization problem [17, 43, 53]. Such model-based methods are heavily dependent on the imaging model and rely on accurate calibration. Thus, they were very limited and the reconstruction quality was low.

To overcome some of these limitations, data-driven algorithms were proposed using deep learning to reconstruct high-quality images from multiplexed measurements. For example, deep learning was used to optimize the alternating direction method of multipliers (ADMM) parameters and reconstruct the image [36]. FlatNet [20, 21] used learned separable transform followed by a Unet [40] architecture which perceptually enhances the resulting image in a generative adversarial network (GAN) approach. GAN is also presented for lensless point spread function (PSF) estimation and robust reconstruction [37]. In [48], a Unet architec-

ture followed by a deep back-projection network (DBPN) [15] was proposed for FZA lensless camera image reconstruction. To address the mismatch between the ideal imaging model and the real-world model, the work in [23] presented multi-Wiener deconvolution networks in multi-scale feature spaces. The research in [25] presented a multi-level image restoration with the pix2pix generative adversarial network. A recent work claimed improved results by incorporating the transformer architecture into the reconstruction model [33].

Diffusion models [9,16,32] are generative models that have gained a lot of popularity in recent years due to their impressive ability to learn the natural image distribution which are used for image generation [12, 31, 38], segmentation [2, 4], inpainting [26], image super-resolution [42], and general image reconstruction [1, 5, 9, 14, 19, 41, 54]. The diffusion model is a parameterized Markov chain that produces samples of a certain data distribution after a predefined T number of steps. In each step of the forward diffusion process, a Gaussian noise is added to the data, such that after a large number of steps, the sample is mapped to an isotropic Gaussian. In the reverse step, a deep neural network is trained to denoise the clean image from the noisy sample. To sample an image, we apply T steps in the reverse direction starting with pure Gaussian noise and denoising it until getting a clean natural image from the learned distribution of the data.

In the context of low-level image restoration, diffusion models were recently used for image restoration of linear inverse problems [8, 10, 19], spatially-variant noise removal [34] and low-light image enhancement and denoising [46,49]. The diffusion method was also presented for a low-light text recognition task [30]. The use of text guidance for conventional imaging reconstruction and enhancement was recently proposed [22, 35, 50]. For non-conventional imaging, such as a flat camera, adopting diffusion models for the recovery process is not trivial and additional adjustments and considerations are required. This work bridges this gap and presents a novel approach to integrating diffusion models for this imaging task.

Latent diffusion model (LDM) [38] is a method for applying the diffusion process in a latent space instead of the pixel space to get a more computationally efficient model for high-resolution images. In this approach, a pre-trained autoencoder consisting of encoder $\mathcal{E}$ and decoder $\mathcal{D}$ is used to train a diffusion model in a low-dimension (latent) space.

The data samples are denoted as $x \sim q(x)$, where q is the data distribution we learn, and the latent sample is obtained by the encoder as $z = \mathcal{E}(x)$. A denoiser network ϵ_θ is trained to predict the added noise (at the backward diffusion step) from the noisy sample z_t at the timestamp $t \in [0, \ldots, T]$. With an additional text input y for text guid-
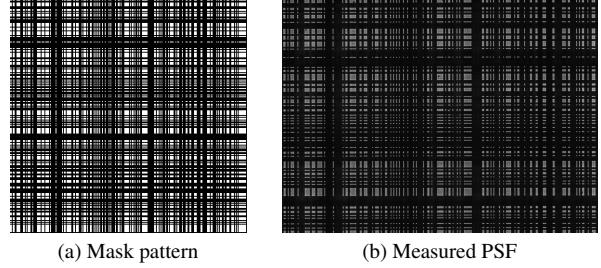

(a) Mask pattern   (b) Measured PSF

Figure 3. **Optical design.** (a) The designed separable mask which was printed on a chrome plate using lithography. (b) The measured PSF by the prototype camera with the coded mask

Table 1. Evaluation and comparison to prior work. Our method outperforms the compared method FlatNet in all metrics. Employing text guidance improves further more the reconstruction results.

method	PSNR↑	SSIM↑	LPIPS↓	CLIP↑
Tikhonov [43]	10.98	0.318	0.736	16.76
flatnet-R [20]	18.58	0.487	0.332	21.53
flatnet-T [20]	18.64	0.518	0.322	21.68
DifuzCam (our)				
without text	<u>20.25</u>	0.601	0.242	22.81
sampled with text	20.20	<u>0.604</u>	<u>0.238</u>	<u>23.50</u>
fine-tuned with text	**20.43**	**0.612**	**0.237**	**23.53**

ance in image generation, the training loss for the LDM is

$$l_{ldm} = \mathbb{E}_{\mathcal{E}(x), \epsilon \sim N(0,\mathbf{I}), t \sim U(0,T)}\left[||\epsilon - \epsilon_\theta(z_t, t, y)||\right]. \quad (2)$$

ControlNet [51] adds an image encoder to control the diffusion process. This control network is initiated as the pre-trained encoder of the diffusion model UNet with additional zero convolutions. The output features of the control network are added to the pre-trained diffusion model features, and due to the zero convolutions, the initial performance of the diffusion model is not degraded. After training, ControlNet weights are optimized such that the added control network features manipulate the diffusion process for the target task. Other methods for controlling the generation process of diffusion models for a specific task were also suggested [13, 28].

3. Proposed Method

We turn to describe our DifuzCam strategy. The flat camera we use employs a similar implementation to previous works [21, 43]. A separable pattern obtained from an outer product of M-sequence binary signals in the length of 255 was used for the amplitude mask. We printed it by lithography on a chrome plate on glass with a thickness of 0.2mm.
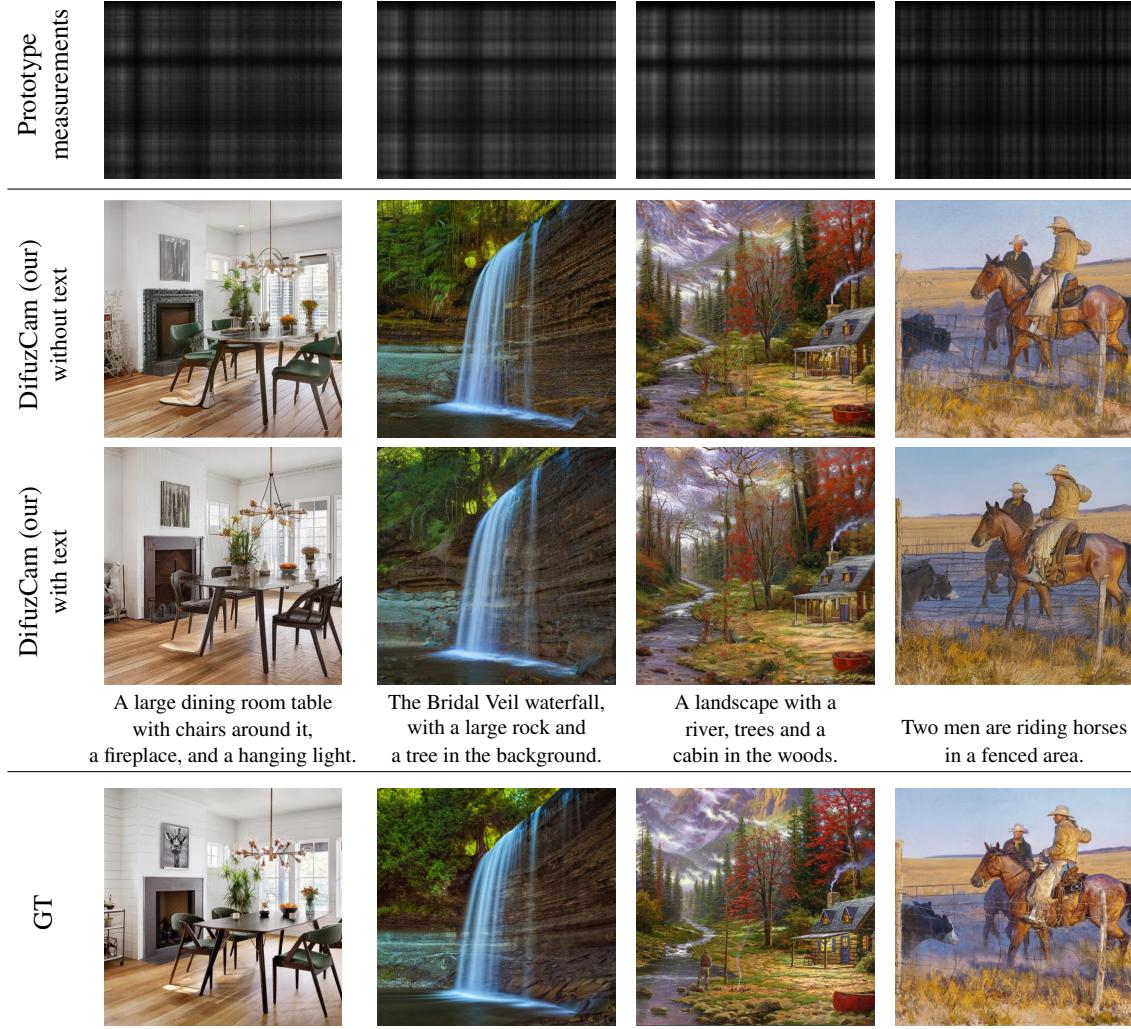
Figure 4. **Qualitative Results.** Examples of reconstruction results for our captured dataset with the prototype camera we designed.

Each feature in the pattern (i.e. a single pinhole) is of size 25 um. Figure 3 shows the mask pattern and the measured camera PSF achieved while the mask is attached to the sensor hot mirror.

The acquired image by a flat camera consists of multiplexed measurements of the light reflected from the scene across the sensor area. The light projections on the sensor create long-range correspondences in the captured images. To convert the image from the projections (i.e. "projection space") to the pixel space of the target image we apply a learned separable linear transformation to the measurements. This transformation is crucial since the input image serves as guidance for the diffusion model process, which was trained and worked in the domain of natural images. The diffusion model is ignorant about the flat camera mask projections on the image, and the control network we use to guide the reconstruction process exhibits better results when operating in the image pixel domain rather than

the long-range projections.

The RAW image captured by the camera (in RGGB Bayer pattern) is split into four color channels: R, G_r, G_b and B. Each channel C_k is linearly transformed as

$$C_k^o = \phi_l^k C_k \phi_r^k, \tag{3}$$

where $k \in [R, G_r, G_b, B]$, each color channel C_k of size $h_i \times w_i$ and $\phi_l \in \mathbb{R}^{h_o \times h_i}$ and $\phi_r \in \mathbb{R}^{w_i \times w_o}$ are two learnable matrices. The output features were stacked onto a single 4-channel tensor $C^o \in \mathbb{R}^{4 \times h_o \times w_o}$.

Since the flat camera image reconstruction is highly ill-posed we utilized a pre-trained diffusion model as our image prior. It is a strong prior for natural images since it is trained on a huge number of samples for the image generation task.

To leverage the diffusion model for our task we need to control its generation process such that we can generate the captured scene from the measurements of the flat
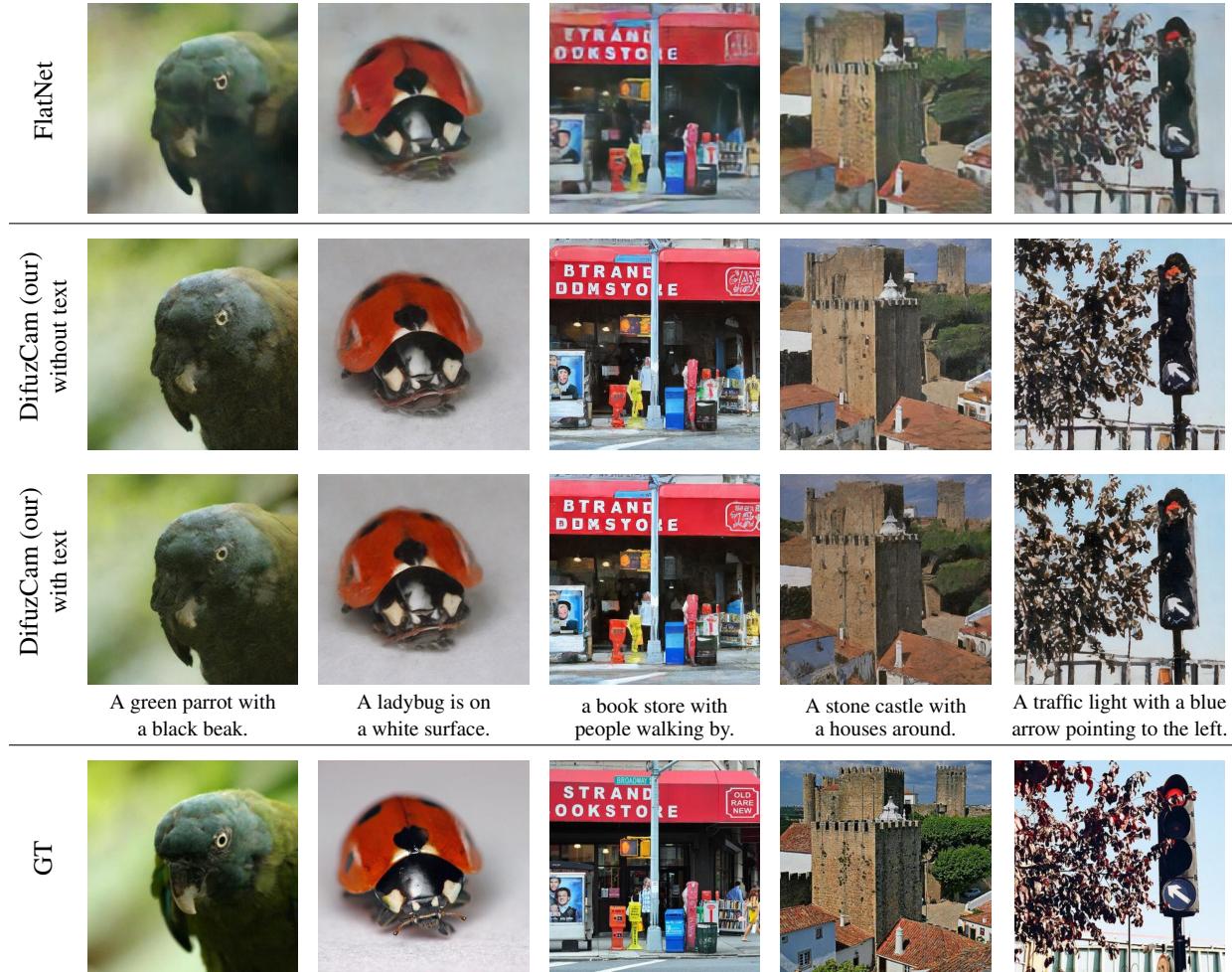
Figure 5. **Results Comparison.** We compare the results of our proposed method to the previous method FlatNet-T [21] on their published data set with their network weights.

camera. To do so we use a ControlNet [51] network $\mathcal{C}_\psi$ which we train for our goal (as presented in Figure 2). This network is initialized as a copy of the encoder of the diffusion model UNet with zero convolutions, such that the pre-trained weights performance is not affected and during training non-zero weights are learned for the reconstruction task.

The input of the control network is the output of the separable transform (C^o) and we use the control network loss

$$l_\mathcal{C} = \mathbb{E}_{\mathcal{E}(x), \epsilon \sim N(0,\mathbf{I}), t \sim U(0,T)} \left[||\epsilon - \epsilon_\theta(z_t, t, y, \mathcal{C}_\psi(C^o))||_2 \right], \tag{4}$$

which is applied for both ψ, the set of parameters of the control network $\mathcal{C}_\psi$, and the learned separable transform weights. The diffusion model parameters θ are pre-trained and fixed.

To guide the training for better results, a separable reconstruction loss term is added to the diffusion conventional loss (Equation (4)). This loss is applied to the output of the separable transformation as

$$l_{sep} = ||I - f_{conv}(C^o)||_2, \tag{5}$$

where f_{conv} is a learned 3×3 convolution layer which maps the 4-channels C^o to 3 channels image, and I is the target (GT) image in RGB channels format. We present in Section 4.2 the improvement and significance of this term.

The diffusion model that we use is a text-guided model for image generation. Thus, we employ this ability to improve the image reconstruction process by giving the model a text description of the captured scene. Giving additional information about the scene content enables the algorithm to have better prior knowledge of the resulting image and reconstruct better images. In this approach the photographer describes the captured scene and this information is input into the reconstruction algorithm. The contribution of the text to the results is presented in Section 4.2.

5

3.1. Data Acquisition and Training

As we train our DifuzCam model (separable transform and control network) in a supervised way, we need pairs of RGB images with their corresponding measurements of the flat camera. Simulating the flat camera imaging process to get realistic measurements such that the trained model will generalize to the real world is very hard since the captured measurements are very dependent on camera properties, alignment, calibration, and mask placement. Because of the small feature size (25um), minor movement of the mask will result in totally different measurements. Due to this sensitivity of the system, we obtained using the optical setup real-world measurements that contain all the imaging properties, including space-variant PSF, diffraction, and non-ideal effects which are hard to simulate such as mask manufacturing inaccuracies, dust, image noise, etc.
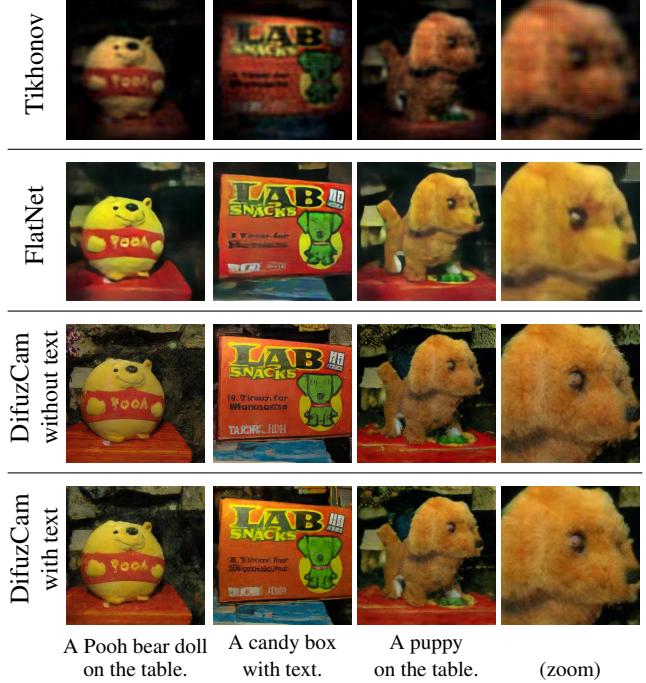
To get a large dataset using our flat camera, we captured images from the LAION-aesthetics dataset [44], which were projected on a PC screen of size 34cm × 34cm at a distance of 60cm from the camera. We used 12ms exposure time and saved the raw Bayer pattern images in 12-bit depth. We used LAION-aesthetics [44] as it consists of a large amount of high-resolution images and their corresponding textual captions. In total, we captured about 55k images. 500 images were saved for testing while the rest were used for training. To compensate for stray light, a black screen with no image projected on it was captured. In the post-processing stage, the measured black levels were subtracted from the captured measurements.

In addition to the screen images, we also capture real objects to show that we are not restricted only to "objects on screen". In this case, we just show the qualitative reconstruction result as we do not have an exact RGB match as in the screen measurement case.

For the pre-trained diffusion model, we used stable-diffusion 2.1 [39]. We trained the model for 500k steps on the captured dataset using the looses in Equation (4) and Equation (2) and learning rate of $5 \cdot 10^{-5}$ with the AdamW optimizer.

4. Experimental Results

Our DifuzCam method was evaluated using several image quality and text similarity metrics. The results of the proposed reconstruction algorithm were compared to the ground through images using PSNR, SSIM [47], and LPIPS [52] metrics. Since we also present a text guidance approach, we measured the CLIP score [36] compared to a GT text description of the captured scene, a metric that evaluates the similarity of an image to a text. For this metric, we used the latest published and most accurate model (ViT-L/14@336px). On the test dataset that we captured, our method achieved 21.89 in PSNR, 0.541 in SSIM, 0.276 in

Figure 6. **Real Scene Results.** Comparison of reconstructions from real scenes measurements with Tikhonov [43], FlatNet-T [21] and Difuzcam (our).

LPIPS, and a CLIP score of 24.38. Figure 4 presents examples of our reconstruction results.

To have a fair comparison to previous works, tests should be performed on the same dataset. Since FlatNet [20] published the dataset of their camera we conducted experiments also on their data to present a valid comparison. Unfortunately, we could not compare to [23, 33] as they did not publish their code or model weight for comparison. The comparisons to [20] are presented quantitatively in Table 1 and visually in Figure 5. Our method achieved superior results in all evaluated metrics for non-text-guided models. Adding a text to the reconstruction process improves the results in the perceptual and textual similarity metrics. Note that when we just add text without fine-tuning the model to use it a minor degradation in PSNR is observed. When we fine-tune the model to be text-guided we get the best improvement (Table 1). Figure 6 presents results for reconstructions of real scenes (not captured from a screen) that are provided in [21] and it compares to Flatnet [21] and Tikhonov [43]. Figure 7 presents real scene reconstructions using our prototype camera.

4.1. Implementation details

In the Laion dataset, the given text captions for the images are not always accurate or relevant. We acknowledge that this noise in the data might harm the results we get in

Table 2. Results and ablation of our method on dataset captured by the prototype camera.

method	PSNR↑	SSIM↑	LPIPS↓	CLIP↑
w/o sep. loss	9.84	0.175	0.666	23.22
w/o text train	21.44	0.512	0.304	22.50
Proposed method	**21.58**	**0.541**	**0.276**	**24.38**

Difuzcam (our) without text	Difuzcam (our) with text	Reference image (not aligned)

A plant with green and yellow leaves.

Black palm trees on a red, orange and yellow background.

Sheep and grass in the field with gray panels background.

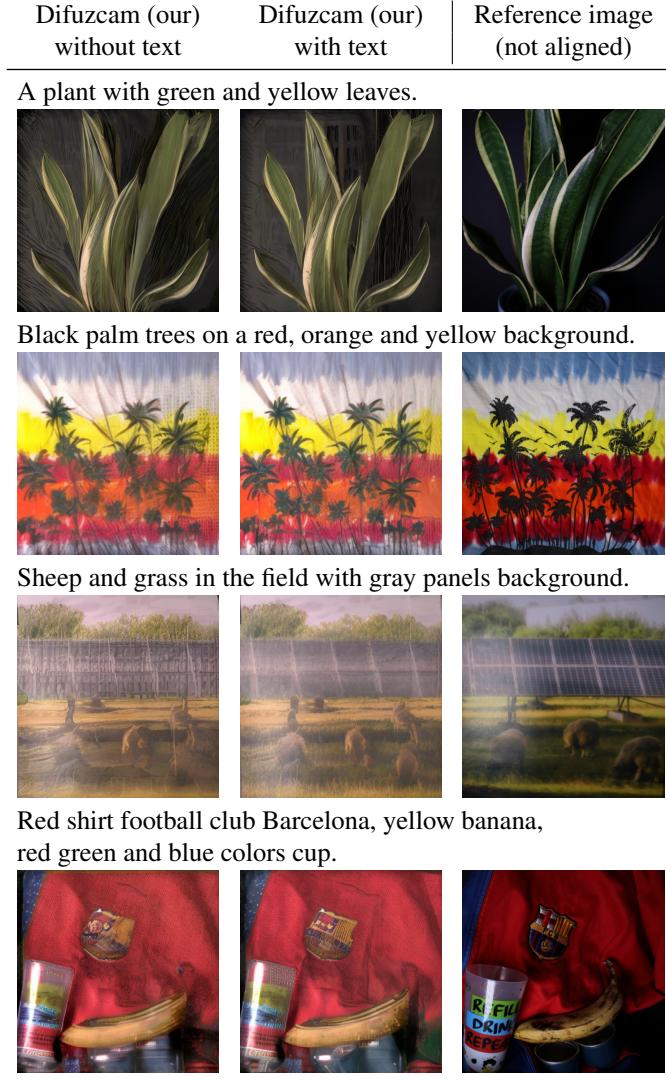Red shirt football club Barcelona, yellow banana, red green and blue colors cup.

Figure 7. **Our Prototype Results.** Real objects were captured with our prototype camera and reconstructed using our proposed method (Difuzcam) with and without text. The reference images were captured with a Canon 80D for visual comparison. Note that they are not accurately aligned with the Difuzcam results.

the training process when using these text captions. Since we identified that these inaccuracies might be critical in the tests, we manually checked the test dataset captions to verify the accuracy and correctness of the data. This verifi-

cation is very important for the text guidance reconstruction results and also for the textual CLIP score evaluation we made. Despite the potential disadvantage of training on incorrect captions, we did not manually verify the training dataset since it is not feasible to manually check such a very large dataset.

To compare our results to FlatNet [20], we trained our method on their published dataset which consists of 10k images for training and 100 for testing. This data does not contain captions to the images. Thus, to train our method with text guidance on this data we use a large language model (LLM) for the auto image captioning process. We used llava1.5 [24] LLM and generated captions for all the images in the data. Here we also might have the problem of incorrect captions, which is also known as LLM hallucinations. Also in this case, the test samples captions were manually verified due to the high importance of the test captions' correctness. For this data we trained the model for 700k steps with a similar optimizer setup to what we mentioned in Section 3.1. We used the Allied Vision 1800 U-500 board-level camera with a pixel size of 2.2um and 5 megapixels overall for the prototype camera.

4.2. Ablations

We present ablation results in Table 2 and Figure 8. First of all, it is noticeable from Table 2 that without our proposed separable loss the reconstructed images are not similar to the target image. We observe that the reconstructed images contain the information of the text caption, according to the high CLIP score, but do not succeed in extracting additional information from the camera measurements for the reconstruction process, i.e., the reconstructions become independent of the input camera measurements. When we do use the separable loss, the measurements are taken into account. Adding text information as input improves the reconstruction even further, compared to the non-text-guided model. The visual ablation images in Figure 8 show that the text captions contribute to the high frequency details in the reconstructed images. When we supply a text caption, the reconstructed image details are aligned with the text. This is noticeable also when a wrong text caption is provided. For example, the reconstruction gains a painting style when the caption mentions a painting and elephant shapes are visible when elephants are described in the caption.

5. Conclusion

A novel method for image reconstruction from flat camera measurements was presented, achieving high quality reconstructions, with and without text guidance. The method leverages the strong capabilities of a pre-trained diffusion model for image prior. Such an approach can be integrated into other imaging systems to improve the reconstructions. Even though we get perceptually pleasant recon-
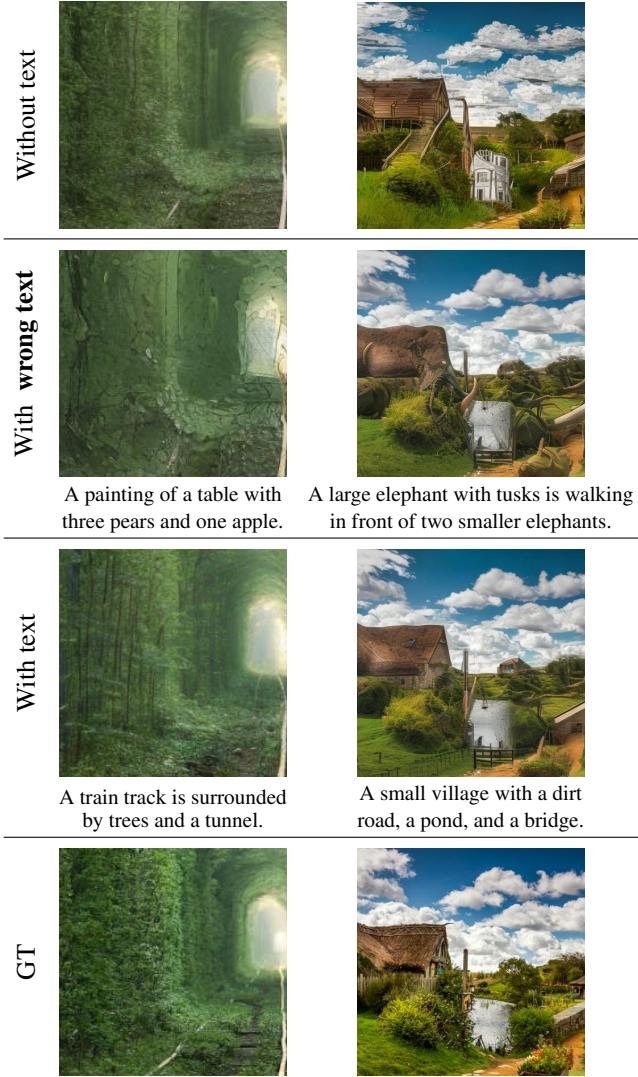
Figure 8. **Ablation Results.** Showing the contribution of the text to the reconstruction. Without text input, the reconstruction is driven by the flat camera measurements only. With text guidance, the reconstructed image details are more similar to the true captured scene. Yet, when a wrong image caption is given, the reconstructed details and high frequencies might be wrong and less compatible with the scene.

structed images, one may notice minor inaccuracies in the reconstructed fine details compared to the ground-through image. Since the imaging method at hand is highly ill-posed, the model learns to generate the missing details, which have been lost in the acquisition process. We therefore do not consider this as a problem but rather a property of the method that improves the reconstruction quality. As we have demonstrated in this work, our approach presents state-of-the-art results compared to previous results and significantly improves the reconstruction abilities of flat cameras.

References

[1] Shady Abu-Hussein, Tom Tirer, and Raja Giryes. Adir: Adaptive diffusion for image reconstruction. *arXiv preprint arXiv:2212.03221*, 2022. 3

[2] Tomer Amit, Tal Shaharbany, Eliya Nachmani, and Lior Wolf. Segdiff: Image segmentation with diffusion probabilistic models. *arXiv preprint arXiv:2112.00390*, 2021. 3

[3] Nick Antipa, Grace Kuo, Reinhard Heckel, Ben Mildenhall, Emrah Bostan, Ren Ng, and Laura Waller. Diffusercam: lensless single-exposure 3d imaging. *Optica*, 5(1):1–9, 2018. 2

[4] Dmitry Baranchuk, Ivan Rubachev, Andrey Voynov, Valentin Khrulkov, and Artem Babenko. Label-efficient semantic segmentation with diffusion models. *arXiv preprint arXiv:2112.03126*, 2021. 3

[5] Georgios Batzolis, Jan Stanczuk, Carola-Bibiane Schönlieb, and Christian Etmann. Conditional image generation with score-based diffusion models. *arXiv preprint arXiv:2111.13606*, 2021. 3

[6] Vivek Boominathan, Jesse K Adams, Jacob T Robinson, and Ashok Veeraraghavan. Phlatcam: Designed phase-mask based thin lensless camera. *IEEE transactions on pattern analysis and machine intelligence*, 42(7):1618–1629, 2020. 2

[7] Vivek Boominathan, Jacob T Robinson, Laura Waller, and Ashok Veeraraghavan. Recent advances in lensless imaging. *Optica*, 9(1):1–16, 2022. 2

[8] Hyungjin Chung, Jong Chul Ye, Peyman Milanfar, and Mauricio Delbracio. Prompt-tuning latent diffusion models for inverse problems. *arXiv preprint arXiv:2310.01110*, 2023. 3

[9] Florinel-Alin Croitoru, Vlad Hondru, Radu Tudor Ionescu, and Mubarak Shah. Diffusion models in vision: A survey. *IEEE Transactions on Pattern Analysis and Machine Intelligence*, 2023. 1, 3

[10] Mauricio Delbracio and Peyman Milanfar. Inversion by direct iteration: An alternative to denoising diffusion for image restoration. *arXiv preprint arXiv:2303.11435*, 2023. 3

[11] Michael J DeWeert and Brian P Farm. Lensless coded aperture imaging with separable doubly toeplitz masks. In *Compressive Sensing III*, volume 9109, pages 180–191. SPIE, 2014. 2

[12] Prafulla Dhariwal and Alexander Nichol. Diffusion models beat gans on image synthesis. *Advances in neural information processing systems*, 34:8780–8794, 2021. 3

[13] Xiaoyue Duan, Shuhao Cui, Guoliang Kang, Baochang Zhang, Zhengcong Fei, Mingyuan Fan,

and Junshi Huang. Tuning-free inversion-enhanced control for consistent image editing. In *Proceedings of the AAAI Conference on Artificial Intelligence*, volume 38, pages 1644–1652, 2024. 3

[14] Ben Fei, Zhaoyang Lyu, Liang Pan, Junzhe Zhang, Weidong Yang, Tianyue Luo, Bo Zhang, and Bo Dai. Generative diffusion prior for unified image restoration and enhancement. In *Proceedings of the IEEE/CVF Conference on Computer Vision and Pattern Recognition*, pages 9935–9946, 2023. 3

[15] Muhammad Haris, Gregory Shakhnarovich, and Norimichi Ukita. Deep back-projection networks for super-resolution. In *Proceedings of the IEEE conference on computer vision and pattern recognition*, pages 1664–1673, 2018. 3

[16] Jonathan Ho, Ajay Jain, and Pieter Abbeel. Denoising diffusion probabilistic models. *Advances in neural information processing systems*, 33:6840–6851, 2020. 3

[17] Yi Hua, Shigeki Nakamura, M Salman Asif, and Aswin C Sankaranarayanan. Sweepcam—depth-aware lensless imaging using programmable masks. *IEEE Transactions on Pattern Analysis and Machine Intelligence*, 42(7):1606–1617, 2020. 2

[18] Gang Huang, Hong Jiang, Kim Matthews, and Paul Wilford. Lensless imaging by compressive sensing. In *2013 IEEE International Conference on Image Processing*, pages 2101–2105. IEEE, 2013. 2

[19] Bahjat Kawar, Michael Elad, Stefano Ermon, and Jiaming Song. Denoising diffusion restoration models. *Advances in Neural Information Processing Systems*, 35:23593–23606, 2022. 3

[20] Salman S Khan, VR Adarsh, Vivek Boominathan, Jasper Tan, Ashok Veeraraghavan, and Kaushik Mitra. Towards photorealistic reconstruction of highly multiplexed lensless images. In *Proceedings of the IEEE/CVF International Conference on Computer Vision*, pages 7860–7869, 2019. 1, 2, 3, 6, 7

[21] Salman Siddique Khan, Varun Sundar, Vivek Boominathan, Ashok Veeraraghavan, and Kaushik Mitra. Flatnet: Towards photorealistic scene reconstruction from lensless measurements. *IEEE Transactions on Pattern Analysis and Machine Intelligence*, 44(4):1934–1948, 2020. 2, 3, 5, 6

[22] Jeongsol Kim, Geon Yeong Park, Hyungjin Chung, and Jong Chul Ye. Regularization by texts for latent diffusion inverse solvers. *arXiv preprint arXiv:2311.15658*, 2023. 3

[23] Ying Li, Zhengdai Li, Kaiyu Chen, Youming Guo, and Changhui Rao. Mwdns: reconstruction in multi-scale feature spaces for lensless imaging. *Optics Express*, 31(23):39088–39101, 2023. 3, 6

[24] Haotian Liu, Chunyuan Li, Qingyang Wu, and Yong Jae Lee. Visual instruction tuning. *Advances in neural information processing systems*, 36, 2024. 7

[25] Muyuan Liu, Xiuqin Su, Xiaopeng Yao, Wei Hao, and Wenhua Zhu. Lensless image restoration based on multi-stage deep neural networks and pix2pix architecture. In *Photonics*, volume 10, page 1274. MDPI, 2023. 3

[26] Andreas Lugmayr, Martin Danelljan, Andres Romero, Fisher Yu, Radu Timofte, and Luc Van Gool. Repaint: Inpainting using denoising diffusion probabilistic models. In *Proceedings of the IEEE/CVF Conference on Computer Vision and Pattern Recognition*, pages 11461–11471, 2022. 3

[27] Jennifer R Miller, Cheng-Yu Wang, Christine D Keating, and Zhiwen Liu. Particle-based reconfigurable scattering masks for lensless imaging. *ACS nano*, 14(10):13038–13046, 2020. 2

[28] Chong Mou, Xintao Wang, Liangbin Xie, Yanze Wu, Jian Zhang, Zhongang Qi, and Ying Shan. T2i-adapter: Learning adapters to dig out more controllable ability for text-to-image diffusion models. In *Proceedings of the AAAI Conference on Artificial Intelligence*, volume 38, pages 4296–4304, 2024. 3

[29] Yusuke Nakamura, Takeshi Shimano, Kazuyuki Tajima, Mayu Sao, and Taku Hoshizawa. Lensless light-field imaging with fresnel zone aperture. In *ITE Technical Report 40.40 Information Sensing Technologies (IST)*, pages 7–8. The Institute of Image Information and Television Engineers, 2016. 2

[30] Cindy M Nguyen, Eric R Chan, Alexander W Bergman, and Gordon Wetzstein. Diffusion in the dark: A diffusion model for low-light text recognition. *arXiv preprint arXiv:2303.04291*, 2023. 3

[31] Alex Nichol, Prafulla Dhariwal, Aditya Ramesh, Pranav Shyam, Pamela Mishkin, Bob McGrew, Ilya Sutskever, and Mark Chen. Glide: Towards photorealistic image generation and editing with text-guided diffusion models. *arXiv preprint arXiv:2112.10741*, 2021. 3

[32] Alexander Quinn Nichol and Prafulla Dhariwal. Improved denoising diffusion probabilistic models. In *International Conference on Machine Learning*, pages 8162–8171. PMLR, 2021. 3

[33] Xiuxi Pan, Xiao Chen, Saori Takeyama, and Masahiro Yamaguchi. Image reconstruction with transformer for mask-based lensless imaging. *Optics Letters*, 47(7):1843–1846, 2022. 3, 6

[34] Naama Pearl, Yaron Brodsky, Dana Berman, Assaf Zomet, Alex Rav Acha, Daniel Cohen-Or, and Dani Lischinski. Svnr: Spatially-variant noise removal with

denoising diffusion. *arXiv preprint arXiv:2306.16052*, 2023. 3

[35] Chenyang Qi, Zhengzhong Tu, Keren Ye, Mauricio Delbracio, Peyman Milanfar, Qifeng Chen, and Hossein Talebi. Tip: Text-driven image processing with semantic and restoration instructions, 2023. 3

[36] Alec Radford, Jong Wook Kim, Chris Hallacy, Aditya Ramesh, Gabriel Goh, Sandhini Agarwal, Girish Sastry, Amanda Askell, Pamela Mishkin, Jack Clark, et al. Learning transferable visual models from natural language supervision. In *International conference on machine learning*, pages 8748–8763. PMLR, 2021. 2, 6

[37] Joshua D Rego, Karthik Kulkarni, and Suren Jayasuriya. Robust lensless image reconstruction via psf estimation. In *Proceedings of the IEEE/CVF Winter Conference on Applications of Computer Vision*, pages 403–412, 2021. 2

[38] Robin Rombach, Andreas Blattmann, Dominik Lorenz, Patrick Esser, and Björn Ommer. High-resolution image synthesis with latent diffusion models. In *Proceedings of the IEEE/CVF conference on computer vision and pattern recognition*, pages 10684–10695, 2022. 1, 2, 3

[39] Robin Rombach, Andreas Blattmann, Dominik Lorenz, Patrick Esser, and Björn Ommer. High-resolution image synthesis with latent diffusion models. In *Proceedings of the IEEE/CVF Conference on Computer Vision and Pattern Recognition (CVPR)*, pages 10684–10695, June 2022. 6

[40] Olaf Ronneberger, Philipp Fischer, and Thomas Brox. U-net: Convolutional networks for biomedical image segmentation. In *Medical image computing and computer-assisted intervention–MICCAI 2015: 18th international conference, Munich, Germany, October 5-9, 2015, proceedings, part III 18*, pages 234–241. Springer, 2015. 2

[41] Chitwan Saharia, William Chan, Huiwen Chang, Chris Lee, Jonathan Ho, Tim Salimans, David Fleet, and Mohammad Norouzi. Palette: Image-to-image diffusion models. In *ACM SIGGRAPH 2022 Conference Proceedings*, pages 1–10, 2022. 3

[42] Chitwan Saharia, Jonathan Ho, William Chan, Tim Salimans, David J Fleet, and Mohammad Norouzi. Image super-resolution via iterative refinement. *IEEE Transactions on Pattern Analysis and Machine Intelligence*, 45(4):4713–4726, 2022. 3

[43] M Salman Asif, Ali Ayremlou, Ashok Veeraraghavan, Richard Baraniuk, and Aswin Sankaranarayanan. Flatcam: Replacing lenses with masks and computation. In *Proceedings of the IEEE International Conference on Computer Vision Workshops*, pages 12–15, 2015. 1, 2, 3, 6

[44] Christoph Schuhmann, Romain Beaumont, Richard Vencu, Cade Gordon, Ross Wightman, Mehdi Cherti, Theo Coombes, Aarush Katta, Clayton Mullis, Mitchell Wortsman, et al. Laion-5b: An open large-scale dataset for training next generation image-text models. *Advances in Neural Information Processing Systems*, 35:25278–25294, 2022. 6

[45] Takeshi Shimano, Yusuke Nakamura, Kazuyuki Tajima, Mayu Sao, and Taku Hoshizawa. Lensless light-field imaging with fresnel zone aperture: quasi-coherent coding. *Applied optics*, 57(11):2841–2850, 2018. 2

[46] Nadav Torem, Roi Ronen, Yoav Y Schechner, and Michael Elad. Complex-valued retrievals from noisy images using diffusion models. In *Proceedings of the IEEE/CVF International Conference on Computer Vision*, pages 3810–3820, 2023. 3

[47] Zhou Wang, Alan C Bovik, Hamid R Sheikh, and Eero P Simoncelli. Image quality assessment: from error visibility to structural similarity. *IEEE transactions on image processing*, 13(4):600–612, 2004. 6

[48] Jiachen Wu, Liangcai Cao, and George Barbastathis. Dnn-fza camera: a deep learning approach toward broadband fza lensless imaging. *Optics Letters*, 46(1):130–133, 2021. 2

[49] Xunpeng Yi, Han Xu, Hao Zhang, Linfeng Tang, and Jiayi Ma. Diff-retinex: Rethinking low-light image enhancement with a generative diffusion model. In *IEEE/CVF International Conference on Computer Vision*, pages 12302–12311, 2023. 3

[50] Erez Yosef and Raja Giryes. Tell me what you see: Text-guided real-world image denoising. *arXiv preprint arXiv:2312.10191*, 2023. 3

[51] Lvmin Zhang, Anyi Rao, and Maneesh Agrawala. Adding conditional control to text-to-image diffusion models. In *Proceedings of the IEEE/CVF International Conference on Computer Vision*, pages 3836–3847, 2023. 2, 3, 5

[52] Richard Zhang, Phillip Isola, Alexei A Efros, Eli Shechtman, and Oliver Wang. The unreasonable effectiveness of deep features as a perceptual metric. In *CVPR*, 2018. 6

[53] Yucheng Zheng, Yi Hua, Aswin C Sankaranarayanan, and M Salman Asif. A simple framework for 3d lensless imaging with programmable masks. In *Proceedings of the IEEE/CVF International Conference on Computer Vision*, pages 2603–2612, 2021. 2

[54] Yuanzhi Zhu, Kai Zhang, Jingyun Liang, Jiezhang Cao, Bihan Wen, Radu Timofte, and Luc Van Gool.

Denoising diffusion models for plug-and-play image restoration. In *Proceedings of the IEEE/CVF Conference on Computer Vision and Pattern Recognition*, pages 1219–1229, 2023. 3

[55] Assaf Zomet and Shree K Nayar. Lensless imaging with a controllable aperture. In *2006 IEEE Computer Society Conference on Computer Vision and Pattern Recognition (CVPR'06)*, volume 1, pages 339–346. IEEE, 2006. 2